

A New VSC HVDC model with IEEE 5 bus system

M.Sujatha¹

¹ PG Student, Department of EEE, JNTUA, Ananthapuramu, Andhra Pradesh, India.

Abstract - A new VSC-HVDC model with IEEE5 bus system is proposed in this paper. The power flow solutions of the new model can be solved using the Newton-Raphson method. The HVDC system is considered as the tap changing transformer because each converter is connection of voltage source converter and its transformer. The proposed approach is make changes in fundamental frequency and its VSC-HVDC modeling. In this VSCs are treated as compound transformer device. In order to step up and step down transformers in which PWM-based inverters control is used. In this two models are presented one is back-to-back and other is Point-to-point model. The power flow of these two models is compared and also introduces a new model with IEEE5 bus system. The power flows of these new model with IEEE5 bus are calculated using Newton-Raphson method. The VSC model takes control properties of PWM control. It considers the inductive and capacitive reactive limits and also switching and ohmic losses.

Key Words: VSC-HVDC system, Newton-Raphson method, PWM control, power flows, HVDC converters.

1. INTRODUCTION

The ever growing need for transmission capacity in current day's power systems has led to increased interest in transmission based on voltage source converter high voltage direct current (VSC- HVDC) technology. In earlier days mercury arc valves are used in power transmission, later the research and investigation on improving the capabilities of HVDC technology resulted in emerging thyristors, which is a solid-state semiconductor device, and introducing as a replacement of mercury arc valves in the 1970s. [2]. It is stated that on March 10, 1977 power was transmitted on the world first Voltage source HVDC transmission system between the Hellsjon and Grangesberg in central Sweden, This scheme was an experimental one rated at only 3 Mw and $\pm 10KV$ [3]. In VSC-HVDC technology, the brands introduced are HVDC-Light ® and Siemens uses the name HVDC-PLUS®.

Among the VSC-based controllers commissioned and installed in several transmission systems around the

world, the VSC-HVDC system, also called HVDC-Light® or HVDC-Plus®, is a recent technology which has demonstrated. The semiconductor valves used at VSC-HVDC stations are IGBTs and Valve firing control is PWM. This PWM (Pulse Width Modulation) is used in order to get high speed control of both active and reactive power. The HVDC Light is the most recent HVDC technology based on Voltage Source Converter (VSC) and extruded DC cabled with power units up to 200 MW[2]. Now it is in its fourth generation, This fourth generation technology is termed as HVDC Light G4 and it has two main advantages as compared to previous generations. The advantages of this HVDC Light G4 are converter losses are in order of 1% as 3% found in early design and harmonic generation is low which uses of AC harmonic filters. The HVDC PLUS shows similar operational characteristics such as it uses multi level converters of the modular type and low switching frequencies.

Most basic VSC-HVDC configurations are back-to-back and point-to-point models. It is used in either mono-polar or bipolar fashions. The mono-polar VSC-HVDC links of two configurations is shown schematically in Fig. 1 [2]. In back-to-back model two VSC are series connected on DC side and in point-to-point model through a DC cable. As shown in Fig. 1 each converter station consists of VSC and its connecting Transformer, The primary and secondary windings of this transformer are connected to high-voltage power grid and to the AC side of the VSC same as if they were two STATCOMs.

The behaviour of New VSC -HVDC model as shown in Fig. 1 can be made by employing two VSC models each should be represented by variable voltage source in addition to a coupling impedance and linked together by mismatch active power constraining equation [5]-[7] and solved using Newton-Raphson method. These modeling issues are useful for such as back-to-back and point-to-point schemes [5], multi-terminal schemes [6], and extension to optimal power flows [7].

The main focus on these schemes is on AC side of the VSC-HVDC links and no DC representation is available. There is a provision for DC representation of VSC-HVDC which is STATCOM's AC voltage is expressed as a function of DC voltage and amplitude modulation ratio. But it is

difficult to represent in this model due to its equivalent voltage source nature. This problem can be solved by using a sequential numerical approach is put in [9] and [10]. To solve the AC part of the network whose VSC-HVDC converters are represented as variable voltage sources in which derived values are added in to a DC conductance matrix for representing the multi-node DC network. This is a full VSC-HVDC power flow solution but due to its sequential iterative approach it losses its strong convergence characteristics of the Newton-Raphson method. The modified approach to solution of multi-terminal VSC-HVDC links is represented in Reference[11] where VSC are considered as lossless and the solution is based on power injections in both the AC and the DC nodes. The power flow calculation in power grid for multi terminal VSC-HVDC schemes which is proposed in reference [12]. This paper introduces a VSC-HVDC model it comprises the phase-shifting and scaling nature of PWM control .It also considers the VSC inductive and capacitive reactive power design limits, switching losses and ohmic losses and also it compares this model with another new model reported in this paper. The power flow back-to-back and point-to-point models are compared and also introduce a new model with IEEE5 bus system. By keeping its strong convergence characteristics, the numerical power flow solution is solved using the Newton- Raphson method.

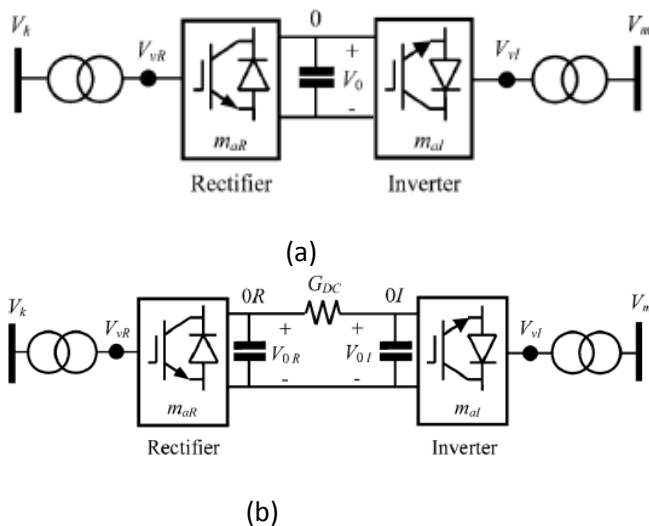


Fig. 1 .VSC-HVDC schematic representation of (a) Back-to-back configuration. (b) Point-to-point configuration.

2. NEW VSC-HVDC MODEL

Two of the VSC models shown in Fig.2 can be used for modeling the fundamental frequency operation of the VSC-HVDC schemes shown in Fig.1. From Fig.2 the middle component of this VSC model is the ideal tap-changing transformer with a complex tap, In this winding connected to node 1 may be denotes to be a AC node and winding connected to node 0 may be denotes to the DC node of the VSC, this will gives a relation which is mostly used in power electronic circuits.

$$\bar{V}_1 = m'_a e^{j\theta} E_{DC} \quad (1)$$

.Where m'_a be the tap magnitude of the ideal tap-changing transformer such as VSCs amplitude modulation coefficient. But this relation is for two level – three phase: $m = \sqrt{3}/2 m_a$

Which takes m_a within violations $0 < m_a < 1$ [13]

Where θ is the phase angle of complex voltage \bar{V}_1 and E_{DC} is DC bus voltage which value 2 in per unit basis.

Actually the VSC can be modeled as two- level or multi- level inverter operating on constant DC voltage E_{DC} , C_{DC} small Dc capacitor is used to support and stabilize the controlled DC voltage E_{DC} which is needed for converter operation[4]. By using electronic processing of the voltage and current waveforms VSC provides either reactive power generation or absorption, according to our requirement PWM control shifts current waveform either lead or lag[4]. The PWM control switching gives B_{sq} according to our requirement which could be capacitive or inductive, where as the other elements in Fig.2 (b) is inductive reactance X_1 representing VSCs interface magnetic and series resistor represents ohmic losses, the shunt resistor such as conductance relating to switching losses in presence of a DC voltage and in parallel with a capacitor.

It is to be stated that R_1 is AC terminal current squared. In this Resistance characteristics which is derived at rated voltage and current where the constant resistance characteristics may be inaccurate so it can be corrected by the quadratic ratio of the actual current to the nominal current.

$$G_0 \left(\frac{I_2^{act}}{I_2^{nom}} \right)^2 \Rightarrow G_{SW} \quad (2)$$

Where G_{SW} be resistive term which exhibits a degree of power behavior.

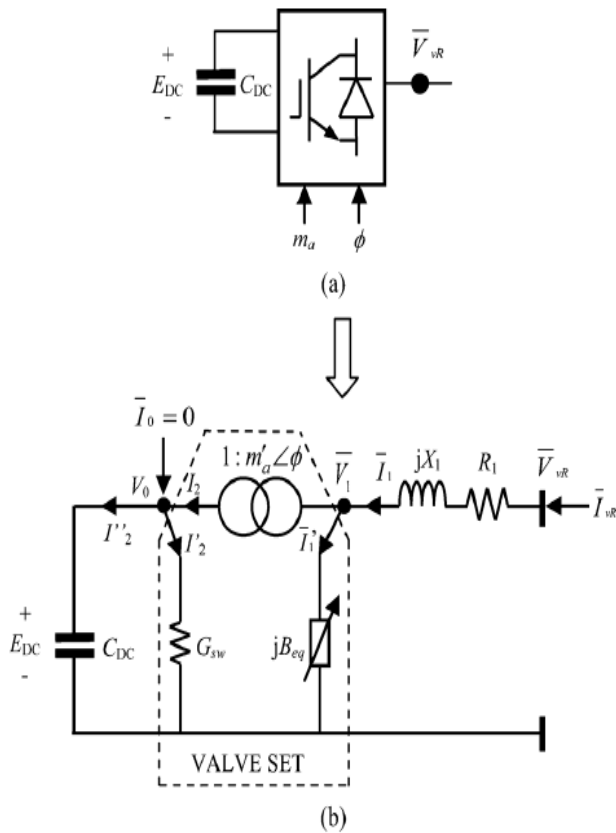


Fig. 2. (a) VSC Schematic representation, (b) VSC equivalent circuit.

It is to be noted that secondary winding current I_2 splits in to I_2 and I_2' . Under steady state operation, the capacitor is assumed to be charged. In this case I_2' would be zero. The steady state model and power flow relation between nodes 1 and 0 will be

$$V_0 I_2 = \bar{V}_1 (\bar{I}_1^* - \bar{I}_1) = \bar{V}_1 \bar{I}_1^* + jB_{eq} V_1^2 \quad (3)$$

The form of equation represents the fundamental operation of the VSC.

$$\begin{pmatrix} \bar{I}_{vR} \\ \bar{I}_0 = 0 \end{pmatrix} = \begin{pmatrix} \bar{V}_1 & -\bar{m}_2 (\cos \phi + j \sin \phi) \bar{V}_1 \\ -\bar{m}_2 (\cos \phi - j \sin \phi) \bar{V}_1 & G_{sw} + \bar{m}_2 (\bar{V}_1 + jB_{eq}) \end{pmatrix} \times \begin{pmatrix} \bar{V}_{vR} \\ V_0 \end{pmatrix} \quad (4)$$

Where \bar{V}_{vR} and \bar{I}_{vR} are the complex voltage and current at node V_R , $\bar{T}_v = \bar{m}_a (\cos \phi + j \sin \phi)$,

$$\bar{T}_v = \bar{T}_i^* \text{ and } \bar{V}_1 = 1/(R_1 + jX_1).$$

Also \bar{I}_0 is a zero injected nodal current at node 0 and V_0 is the voltage at DC bus.

3. POWER FLOW MODEL BACK TO BACK VSC-HVDC

By using the Newton-Raphson method, The linearized equation corresponding to the power flow solution of the back-to-back VSC-HVDC, is calculated in this section.

A. Back-to-Back VSC-HVDC Nodal Power Equations

By following some algebra The nodal active and reactive for the rectifier are arrived at.

$$\begin{aligned} P_{vR} &= G_{1R} V_{vR}^2 - \bar{m}_{aR} V_{vR} V_{oR} \\ &[G_{1R} \cos(\theta_{vR} - \theta_{oR} - \phi_R) + B_{1R} \sin(\theta_{vR} - \theta_{oR} - \phi_R)] \\ Q_{vR} &= -B_{1R} V_{vR}^2 - \bar{m}_{aR} V_{vR} V_{oR} \\ &[G_{1R} \sin(\theta_{vR} - \theta_{oR} - \phi_R) - B_{1R} \sin(\theta_{vR} - \theta_{oR} - \phi_R)] \\ P_{oR} &= (\bar{m}_{aR}^2 G_{1R} + G_{swR}) V_{oR}^2 - \bar{m}_{aR} V_{vR} V_{oR} \\ &[G_{1R} \cos(\theta_{oR} - \theta_{vR} + \phi_R) + B_{1R} \sin(\theta_{oR} - \theta_{vR} + \phi_{vR})] \\ Q_{oR} &= -\bar{m}_{aR}^2 (B_{1R} + B_{1eqR}) V_{oR}^2 - \bar{m}_{aR} V_{vR} V_{oR} \\ &[G_{1R} \sin(\theta_{oR} - \theta_{vR} + \phi_R) + B_{1R} \cos(\theta_{oR} - \theta_{vR} + \phi_R)] \end{aligned} \quad (6)$$

Similarly another set of equations for Inverter

$$\begin{aligned} P_{vI} &= G_{1I} V_{vI}^2 - \bar{m}_{aI} V_{vI} V_{oI} \\ &[G_{1I} \cos(\theta_{vI} - \theta_{oI} - \phi_I) + B_{1I} \sin(\theta_{vI} - \theta_{oI} - \phi_I)] \\ Q_{vI} &= -B_{1I} V_{vI}^2 - \bar{m}_{aI} V_{vI} V_{oI} \\ &[G_{1I} \sin(\theta_{vI} - \theta_{oI} - \phi_I) - B_{1I} \sin(\theta_{vI} - \theta_{oI} - \phi_I)] \\ P_{oI} &= (\bar{m}_{aI}^2 G_{1I} + G_{swI}) V_{oI}^2 - \bar{m}_{aI} V_{vI} V_{oI} \\ &[G_{1I} \cos(\theta_{oI} - \theta_{vI} + \phi_I) + B_{1I} \sin(\theta_{oI} - \theta_{vI} + \phi_I)] \\ Q_{oI} &= -\bar{m}_{aI}^2 (B_{1I} + B_{1eqI}) V_{oI}^2 - \bar{m}_{aI} V_{vI} V_{oI} \\ &[G_{1I} \sin(\theta_{oI} - \theta_{vI} + \phi_I) + B_{1I} \cos(\theta_{oI} - \theta_{vI} + \phi_I)] \end{aligned} \quad (7)$$

$$\begin{pmatrix} \bar{S}_{vR} \\ \bar{S}_0 \end{pmatrix} = \begin{pmatrix} \bar{V}_{vR} & \mathbf{0} \\ \mathbf{0} & V_0 \end{pmatrix} \begin{pmatrix} \bar{I}_{vR}^* \\ \bar{I}_0^* \end{pmatrix}$$

$$\begin{bmatrix} \bar{V}_{vR} & \mathbf{0} \\ \mathbf{0} & V_0 \end{bmatrix} \left\{ \begin{pmatrix} \bar{Y}_1^* & -\dot{m}_2 (\cos \phi + j \sin \phi) \bar{Y}_1^* \\ -\dot{m}_2 (\cos \phi - j \sin \phi) \bar{Y}_1^* & G_{sw} + \dot{m}_2^2 (\bar{Y}_1^* + j B_{eq}) \end{pmatrix} \begin{pmatrix} \bar{V}_{vR}^* \\ V_0 \end{pmatrix} \right\} \quad (5)$$

$$\begin{bmatrix} \Delta P_{vR} \\ \Delta Q_{vR} \\ \dots \\ \Delta P_{vl} \\ \Delta Q_{vl} \\ \dots \\ \Delta P_{vl} \\ \Delta Q_{vl} \\ \dots \\ \Delta P_{oR-vR} \\ \Delta Q_{oR-vR} \\ \dots \\ \Delta P_{oI-vI} \\ \Delta Q_{oI-vI} \end{bmatrix}^{(r)}$$

=

$$\begin{bmatrix} \frac{\partial P_{vR}}{\partial \theta_{vR}} \left(\frac{\partial P_{vR}}{\partial V_{vR}} \right) V_{vR} & \mathbf{0} & \mathbf{0} & \frac{\partial P_{vR}}{\partial \theta_0} & \mathbf{0} & \frac{\partial P_{vR}}{\partial \phi_R} & \frac{\partial P_{vR}}{\partial B_{eqR}} & \mathbf{0} & \mathbf{0} \\ \frac{\partial Q_{vR}}{\partial \theta_{vR}} \left(\frac{\partial Q_{vR}}{\partial V_{vR}} \right) V_{vR} & \frac{\partial P_{vl}}{\partial \theta_{vl}} \left(\frac{\partial P_{vl}}{\partial \dot{m}_{al}} \right) \dot{m}_{al} & \frac{\partial P_{vl}}{\partial \theta_{vl}} \left(\frac{\partial P_{vl}}{\partial \dot{m}_{al}} \right) \dot{m}_{al} & \frac{\partial Q_{vR}}{\partial \theta_0} & \mathbf{0} & \frac{\partial Q_{vR}}{\partial \phi_R} & \frac{\partial Q_{vR}}{\partial B_{eqR}} & \frac{\partial P_{vl}}{\partial \phi_I} & \frac{\partial P_{vl}}{\partial B_{eqI}} \\ \mathbf{0} & \frac{\partial Q_{vl}}{\partial \phi_I} & \frac{\partial Q_{vl}}{\partial B_{eqI}} \\ \mathbf{0} & \frac{\partial P_{oI}}{\partial \phi_I} & \frac{\partial P_{oI}}{\partial B_{eqI}} \\ \frac{\partial P_{oR-vR}}{\partial \theta_{vR}} \left(\frac{\partial P_{oR-vR}}{\partial V_{vR}} \right) V_{vR} & \frac{\partial P_{oI}}{\partial \theta_{vl}} \left(\frac{\partial P_{oI}}{\partial \dot{m}_{al}} \right) \dot{m}_{al} & \frac{\partial P_{oI}}{\partial \theta_{vl}} \left(\frac{\partial P_{oI}}{\partial \dot{m}_{al}} \right) \dot{m}_{al} & \frac{\partial P_{oR}}{\partial \theta_0} & \mathbf{0} & \frac{\partial P_{oR}}{\partial \phi_R} & \frac{\partial P_{oR}}{\partial B_{eqR}} & \frac{\partial P_{oI}}{\partial \phi_I} & \frac{\partial P_{oI}}{\partial B_{eqI}} \\ \mathbf{0} & \mathbf{0} & \mathbf{0} & \mathbf{0} & \mathbf{1} & \mathbf{0} & \mathbf{0} & \mathbf{0} & \mathbf{0} \\ \frac{\partial P_{oR-vR}}{\partial \theta_{vR}} \left(\frac{\partial P_{oR-vR}}{\partial V_{vR}} \right) V_{vR} & \mathbf{0} & \mathbf{0} & \frac{\partial P_{oR-vR}}{\partial \theta_0} & \mathbf{0} & \frac{\partial P_{oR-vR}}{\partial \phi_R} & \frac{\partial P_{oR-vR}}{\partial B_{eqR}} & \mathbf{0} & \mathbf{0} \\ \frac{\partial Q_{oR-vR}}{\partial \theta_{vR}} \left(\frac{\partial Q_{oR-vR}}{\partial V_{vR}} \right) V_{vR} & \frac{\partial P_{oI-vI}}{\partial \theta_{vl}} \left(\frac{\partial P_{oI-vI}}{\partial \dot{m}_{al}} \right) \dot{m}_{al} & \frac{\partial P_{oI-vI}}{\partial \theta_{vl}} \left(\frac{\partial P_{oI-vI}}{\partial \dot{m}_{al}} \right) \dot{m}_{al} & \frac{\partial Q_{oR-vR}}{\partial \theta_0} & \mathbf{0} & \frac{\partial Q_{oR-vR}}{\partial \phi_R} & \frac{\partial Q_{oR-vR}}{\partial B_{eqR}} & \frac{\partial P_{oI-vI}}{\partial \phi_I} & \frac{\partial P_{oI-vI}}{\partial B_{eqI}} \\ \mathbf{0} & \frac{\partial Q_{oI-vI}}{\partial \phi_I} & \frac{\partial Q_{oI-vI}}{\partial B_{eqI}} \\ \mathbf{0} & \frac{\partial Q_{oI-vI}}{\partial \phi_I} & \frac{\partial Q_{oI-vI}}{\partial B_{eqI}} \end{bmatrix}^{(r)} X \begin{bmatrix} \Delta \theta_{vR} \\ \Delta V_{vR} \\ \dots \\ \Delta \theta_{vl} \\ \Delta \dot{m}_{al} \\ \dots \\ \theta_0 \\ \Delta V_{vl} \\ V_{vl} \\ \dots \\ \Delta \phi_R \\ \Delta B_{eqR} \\ \dots \\ \Delta \phi_I \\ \Delta B_{eqI} \end{bmatrix}^{(r)}$$

From Fig.1 it shows that both converters are connected on their DC side to a common bus 0, it is clear that buses 0R and 0I are at same bus in this back-to-back VSC-HVDC application.

B. Back-to-Back VSC-HVDC Linearized Equations

The solution of generation and load pattern can be carried out by using Newton-Raphson method.

Because these nodal power equations are non Linear.

These calculated powers are obtained from the nodal equations (6) and (7). In order to regulate power on DC side a rectifier is used and to regulate voltage smagnitude on its AC side an inverter is used. In order to stabilize the DC voltage a small DC capacitor is used on each of the two VSCs which is needed for converter operation.

In order to obtain zero reactive power at node 0 these constraining equations are used. Hence, there is additional two state variables are available such as equivalent susceptances of the two VSCs.

Linearization of equations (6) and (7) around the base operating points,

$(\theta_{vR}^{(0)}, V_{vR}^{(0)}, \theta_{vI}^{(0)}, V_{vI}^{(0)}, \theta_0^{(0)}, m_{aI}^{(0)}, \phi_R^{(0)}, B_{eqR}^{(0)}, \phi_I^{(0)}, B_{eqI}^{(0)})$ is used to regulate voltage magnitude at the inverters AC side and to control power on the DC side using \dot{m}_a . Treat the node 0 as a PV-like bus that V_0 is kept at constant value.

The corresponding equations is arranged as shown in (8) of the page.

I. Mismatch Power Terms and Control Variables:

The mismatch power is obtained from the difference between the net power and calculated powers at buses V_R, V_I and 0.

$$\Delta P_{vR} = P_{vR,net} - P_{vR,cal} = (P_{vR,gen} - P_{vR,load}) - P_{vR,cal}$$

$$\Delta Q_{vR} = Q_{vR,net} - Q_{vR,cal} = (Q_{vR,gen} - Q_{vR,load}) - Q_{vR,cal}$$

$$\Delta P_{oR} = P_{oR,net} - P_{oR,cal} = (P_{oR,gen} - P_{oR,load}) - P_{oR,cal}$$

$$\Delta P_{oR-vR} = P_{oR-vR,reg} - P_{oR-vR,cal}$$

$$\Delta Q_{oR-vR} = 0 - Q_{oR-vR,cal}$$

$$\Delta P_{vI} = P_{vI,net} - P_{vI,cal} = (P_{vI,gen} - P_{vI,load}) - P_{vI,cal}$$

$$\Delta Q_{vI} = Q_{vI,net} - Q_{vI,cal} = (Q_{vI,gen} - Q_{vI,load}) - Q_{vI,cal}$$

$$\Delta P_{oI} = P_{oI,net} - P_{oI,cal} = (P_{oI,gen} - P_{oI,load}) - P_{oI,cal}$$

$$\Delta Q_{oI} = Q_{oI,net} - Q_{oI,cal} = (Q_{oI,gen} - Q_{oI,load}) - Q_{oI,cal}$$

$$\Delta P_{oI-vI} = P_{oI-vI,reg} - P_{oI-vI,cal}$$

$$\Delta Q_{oI-vI} = 0 - Q_{oI-vI,cal} \quad (9)$$

In this application, the reactive power targets are set to zero and $P_{oR-vR,reg} = P_{oI-vI,reg}$

II. State Variables and Increments:

The state variables are updated at iteration (r), as follows:

$$\theta_{vR}^{(r)} = \theta_{vR}^{(r-1)} + \Delta\theta_{vR}^{(r)}$$

$$V_{vR}^{(r)} = V_{vR}^{(r-1)} + \left(\frac{\Delta V_{vR}^{(r)}}{V_{vR}^{(r)}}\right) V_{vR}^{(r-1)}$$

$$\theta_{vI}^{(r)} = \theta_{vI}^{(r-1)} + \Delta\theta_{vI}^{(r)}$$

$$\theta_0^{(r)} = \theta_0^{(r-1)} + \Delta\theta_0^{(r)}$$

$$\dot{m}_{aI}^{(r)} = \dot{m}_{aI}^{(r-1)} + \left(\frac{\Delta \dot{m}_{aI}^{(r)}}{\dot{m}_{aI}^{(r)}}\right) \cdot \dot{m}_{aI}^{(r-1)}$$

$$\phi_R^{(r)} = \phi_R^{(r-1)} + \Delta\phi_R^{(r)}$$

$$\phi_I^{(r)} = \phi_I^{(r-1)} + \Delta\phi_I^{(r)}$$

$$B_{eqR}^{(r)} = B_{eqR}^{(r-1)} + \Delta B_{eqR}^{(r)}$$

$$B_{eqI}^{(r)} = B_{eqI}^{(r-1)} + \Delta B_{eqI}^{(r)}$$

(9)

III. Practical implementations:

Control Strategy: As illustrated in Fig.1(a) the voltage V_0 is kept as constant t by using a small DC capacitor bank of each of value C_{DC} while the VSC acting as a rectifier and it is connected between sending bus VR and receiving bus 0 with one side is connected to VSC's AC bus and the other side VSC's DC bus. The relationship of maximum and minimum values of voltage magnitude within the system is,

$$|V_{vR}| = m_{aR} E_{DC} - \sqrt{R_1^2 + X_1^2} \cdot |\bar{I}_1| \quad (11)$$

The modulation index values lies within bounds $0 < m_{aR} < 1$, but in practice actual modulation ratio is lower than 0.5. The VSC current upper design limits $|\bar{I}_1| < I_{VSCmax}$ and the upper and lower ceilings of B_{eqR} are obtained from the design values of E_{DC} and $\pm Q_{VSC}$: $B_{eqR+} = +Q_{VSC}/E_{DC}^2$ and $B_{eqR-} = -Q_{VSC}/E_{DC}^2$. Similar relationship exists in VSC inverter which is connected between sending bus, and receiving bus 0.

Simplifying Assumptions:

The two resistors consists of internal losses of the VSCs and the inductor represents their interface magnetic and it is constant parameter. The phase angle at is independent of circuit parameters. Because ideal phase shifter decouples angle decouples angle wise. Hence according to application of tis paper it makes a zero phase angle voltage initialization for this bus, In rectangular coordinates of voltage its imaginary part does not exist,

$$\bar{V}_0 = V_0 < 0 \rightarrow \bar{V}_0 = e_0 + j0 \rightarrow V_0 = e_0$$

Initial Parameters and Limits:

The initialization of three sets of VSC parameters are: The amplitude modulation ratios; the phase angles and the equivalent susceptances. Set the amplitude modulation ratio $\sqrt{3/2}$ and phase angles at . Assume the VSCs to operate in linear regions, with actual modulation ratios takes positive maximum values and minimum value is at 0. =, ut actual power system operation conditions its value is lower than 0.5[13]. The phase angles has no limits and the equivalent susceptances are lie within range.

C. LTC Transformer Model

The nodal admittance matrix of the LTC transformer which is connected between buses K and V_{vR}

$$\begin{pmatrix} \bar{I}_k \\ \bar{I}_{vR} \end{pmatrix} = \begin{pmatrix} \bar{Y}_t & -T\bar{Y}_t \\ -T\bar{Y}_t & -T^2\bar{Y}_t \end{pmatrix} \begin{pmatrix} \bar{V}_k \\ \bar{V}_{vR} \end{pmatrix} \quad (12)$$

linearization of (13) around base operating point is suitable to regulate voltage magnitude at bus.

The above equation describes the LTC connected between buses K and V_R , similar relation would exists in between buses Vi and M only by changing the subscriptions.

The LTC transformer active and reactive power expressions at bus k and V_R .

$$\begin{aligned} P_k &= G_t V_k^2 - TV_k V_{vR} \\ [G_t \cos(\theta_k - \theta_{vR}) + B_t \sin(\theta_k - \theta_{vR})] \\ Q_k &= -B_t V_k^2 - TV_k V_{vR} \\ [G_t \sin(\theta_k - \theta_{vR}) - B_t \cos(\theta_k - \theta_{vR})] \\ P_{vRt} &= G_t T^2 V_{vR}^2 - TV_k V_{vR} \\ [G_t \cos(\theta_{vR} - \theta_t) + B_t \sin(\theta_{vR} - \theta_K)] \\ Q_{vRt} &= -B_t T^2 V_{vR}^2 - TV_k V_{vR} \\ [G_t \sin(\theta_{vR} - \theta_K) - \cos(\theta_{vR} - \theta_K)] \end{aligned} \quad (13)$$

Where V_k and θ_K are the phase angle and complex voltage of voltage \bar{V}_k . Similarly V_{vR} and θ_{vR} are the phase angle and complex voltage of voltage \bar{V}_{vR} . Also G_t and B_t are real and imaginary parts of Y_t .

In order to regulate voltage magnitude, LTC tap is used at bus k and V_R .

For example, linearization of (13) around operating points is suitable to regulate voltage at bus K

$$\begin{bmatrix} \Delta P_k \\ \Delta Q_k \\ \Delta P_{vRt} \\ \Delta Q_{vRt} \end{bmatrix}^{(r)} = \begin{bmatrix} \frac{\partial P_k}{\partial \theta_K} \left(\frac{\partial P_k}{\partial T} \right) T & \frac{\partial P_k}{\partial \theta_{vR}} \left(\frac{\partial P_k}{\partial V_{vR}} \right) V_{vR} \\ \frac{\partial Q_k}{\partial \theta_K} \left(\frac{\partial Q_k}{\partial T} \right) T & \frac{\partial Q_k}{\partial \theta_{vR}} \left(\frac{\partial Q_k}{\partial V_{vR}} \right) V_{vR} \\ \frac{\partial P_{vRt}}{\partial \theta_K} \left(\frac{\partial P_{vRt}}{\partial T} \right) T & \frac{\partial P_{vRt}}{\partial \theta_{vR}} \left(\frac{\partial P_{vRt}}{\partial V_{vR}} \right) V_{vR} \\ \frac{\partial Q_{vRt}}{\partial \theta_K} \left(\frac{\partial Q_{vRt}}{\partial T} \right) T & \frac{\partial Q_{vRt}}{\partial \theta_{vR}} \left(\frac{\partial Q_{vRt}}{\partial V_{vR}} \right) V_{vR} \end{bmatrix}^{(r)} \begin{bmatrix} \Delta \theta_K \\ \Delta T \\ \Delta \theta_{vR} \\ \Delta V_{vR} \end{bmatrix}^{(r)}$$

In order to represent the full back-to-back VSC-HVDC as shown in Fig 1 (a), an interfacing of two back-to-back VSCs and two LTC VSCs are needed; it requires an expansion of (8) to add the buses K and m, where self terms of V_R in (8) and (14) are added together. Similarly the self terms of Vi and m in (8) and (14) are also added together.

The linearization of LTC introduces an additional:

$\Delta P_k, \Delta Q_k, \Delta P_{vRt}, \Delta Q_{vRt}$ and $\Delta P_m, \Delta Q_m, \Delta P_{vlt}, \Delta Q_{vlt}$. The power mismatches of two LTC tap coincides with AC nodes of two VSCs, are added together:

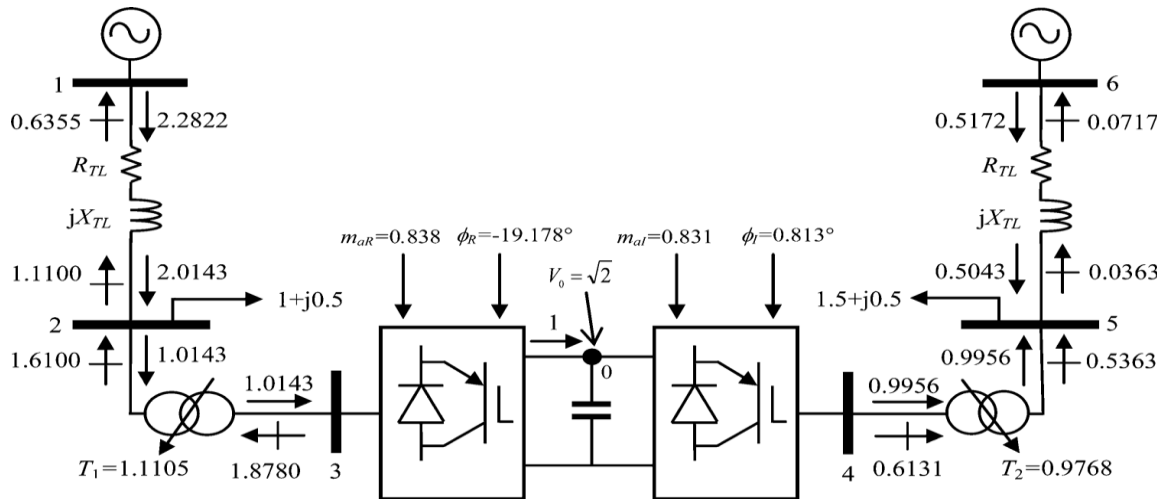


Fig.3. Back-to-back VSC-HVDC consists two equivalent AC sub-systems .The following parameters are used

- (i) Transmission line 1 and 2: $R_{TL} = 0.05 \text{ p.u.}$ and $X_{TL} = 0.10 \text{ p.u.}$; (ii) VSC 1 and VSC 2 series resistance and reactance: 0.001 p.u., 0.01 p.u. , ; (iii) VSC 1 and VSC 2 initial shunt conductance for switching loss calculation $G_{sw} = 0.01 \text{ P.U.}$; (iv) LTC 1 and 2 series reactance :0.06 p.u; (v) active and reactive power load at bus 2: 1p.u and 0.5 p.u; (vi) active and reactive power at bus 5: 1.5 p.u and 0.5 p.u.

Table 1

Power flow voltage solution

Nodes	1	2	3	0	4	5	6
V(p.u)	1.02	1.00	1.01	1.4142	1.01	1.00	1.02
$\theta(\text{deg})$	0	-14.67	-18.51	-	0.29	-3.02	0

Table 2

Tap values for the two VSCs and two LTCs

VSC	1	2	LTC	1	2
m_a	$0.838 \angle -19.178^\circ$	$0.831 \angle 0.813^\circ$	Tap	1.1105	0.9768

ΔP_{vR} and ΔP_{vRt} ; ΔQ_{vR} and ΔQ_{vRt} ;

ΔP_{vi} and ΔP_{vit} ; ΔQ_{vi} and ΔQ_{vit} . At iteration (r) , the additional state variables are calculated such as $\theta_k^{(r)}$, $V_k^{(r)}$, $\theta_m^{(r)}$, $V_m^{(r)}$. By using the tap of the LTC which is connected between buses k and V_R is controlled voltage in either of the bus k or bus V_R which is associated with state variable $T^{(k)}$.which modified as either $V_K^{(r)}$ or $V_{vR}^{(r)}$ depending on which LTC tap acts. Similar relation exists for LTC transformer which is connected between m and V_I .

D. Back-to-Back VSC-HVDC Test Cases

The test case presented in this section as shown in Fig.3 where VSC-HVDC link is used to interconnect two independent AC systems.

In this example the two VSCs are connected on their AC side through LTC Transformer operating off their nominal tap positions. As shown in Fig.3 the power leaving the rectifier is set at 1 p.u using connection then each AC subsystem require its own slack bus. Buses 1 and 6 are designed as slack bus and Bus 0 is DC-like bus. The active and reactive power on each generator contributes to 2.2822 p.u. and 0.5172 p.u. of active power respectively.

The phase angle voltages at bus 1 provide reference for phase angle voltages at 2 and 3 buses similarly bus 6. Reference for 4 and 5 buses. The voltage solution shown in table.1 VSC1 and two VSCs are connected between buses 3 and 4 through DC bus 0 where voltage is regulated at 1.414 p.u. Since it is asynchronous the active power occurred in VSC connected to bus 3 are at 1.43% with 0.99% switching losses and remaining conduction losses. At bus 3 delivers 1.878 p.u of reactive power in this 0.5 p.u is connected to load at bus2 and 0.6355 p.u absorbed by slack bus 1 and remaining is used for losses which occurred in between node 1 and 2. similarly the active power loss at bus4 at 0.44% switching losses 0.3% and conduction losses 0.14% and reactive power at bus 40.6131 similarly 0.5 p.u reactive power connected load at bus 5 and remaining for losses. The complex taps corresponds to two VSCs as shown in table.2. The

susceptances of VSC 1 and 2 produce 1.9226 p.u. and 0.6383 p.u. of reactive power. The solution converges in 7 iterations to a mismatch tolerance of 10^{-12} .

4. POWER FLOW MODEL: POINT-TO-POINT VSC-HVDC

The nodal power equations for the rectifier which is developed and is used in this model, where as for inverter it should be calculated. In this section the model consists of the VSC model in series with a DC cable combined VSC cable DC representation.

A. Combined VSC-DC cable Representation

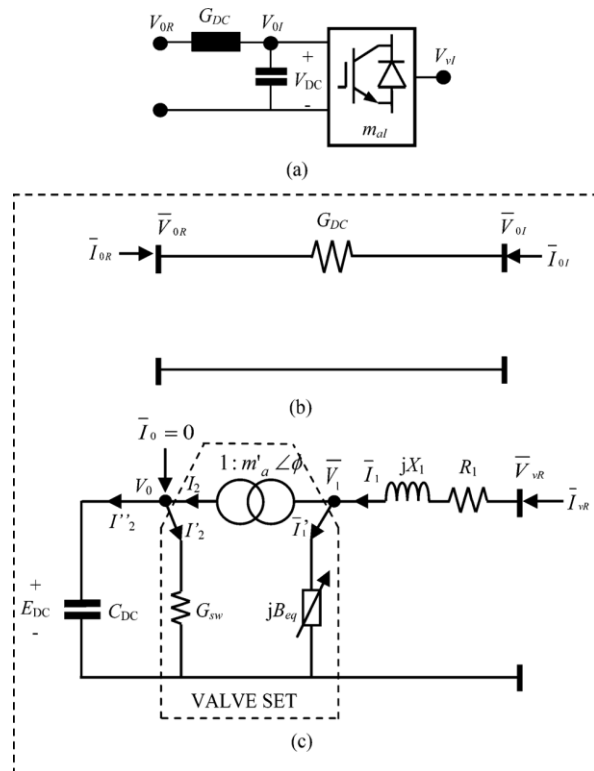


Fig. 4. (a) VSC-DC cable schematic representation. (b) Cable equivalent circuit. (c) VSC equivalent circuit.

The fundamental frequency operation of combines a VSC-HVDC model and a DC cable as shown in Figure 4.

The VSC admittance matrix (4), with changed subscripts to represent the inverter, and that of a DC cable are combined for following representation

(18)

$$\begin{pmatrix} \bar{I}_{VI} \\ \bar{I}_{OI} \\ \bar{I}_{OR} \end{pmatrix} = \begin{pmatrix} \bar{Y}_1 & -m'_{aI} \angle -\phi_I \bar{Y}_1 & 0 \\ -m'_{aI} \angle -\phi_I \bar{Y}_1 & m'_{aI} z^2 (\bar{Y}_1 + jB_{eq}) + G_{sw} + \bar{Y}_{DC} & -\bar{Y}_{DC} \\ 0 & -\bar{Y}_{DC} & \bar{Y}_{DC} \end{pmatrix} \times \begin{pmatrix} \bar{V}_{VI} \\ \bar{V}_{OI} \\ \bar{V}_{OR} \end{pmatrix} \quad (15)$$

Mathematical elimination of node OI gives the equation 17

A. Point-to-Point VSC-HVDC Nodal Power Equations

By making use of nodal matrix 17 the power flow model is calculated similar to (5) where as for inverter side it should be arrived at

$$P_{VI} = G_{eq1} V_{VI}^2 - m'_{aI} V_{VI} V_{OR} [G_{eq1DC} \cos(\theta_{VI} - \theta_{OR} - \phi_I) + B_{eq1DC} \sin(\theta_{VI} - \theta_{OR} - \phi_I)]$$

$$Q_{VI} = -B_{eq1} V_{VI}^2 - m'_{aI} V_{VI} V_{OR} [G_{eq1DC} \sin(\theta_{VI} - \theta_{OR} - \phi_I) - B_{eq1DC} \cos(\theta_{VI} - \theta_{OR} - \phi_I)]$$

$$P_{OR} = G_{eq0} V_{OR}^2 - m'_{aI} V_{VI} V_{OR} [G_{eq1DC} \cos(\theta_{OR} - \theta_{VI} + \phi_I) + B_{eq1DC} \sin(\theta_{OR} - \theta_{VI} + \phi_I)]$$

$$Q_{OR} = -B_{eq0} V_{OR}^2 - m'_{aI} V_{VI} V_{OR} [G_{eq1DC} \sin(\theta_{OR} - \theta_{VI} + \phi_I) - B_{eq1DC} \cos(\theta_{OR} - \theta_{VI} + \phi_I)]$$

B. Point-to-Point VSC-HVDC Linearized System of Equations:

The combine solution of (6) and (18) gives the solution of the point-to-point VSC-HVDC, for a set of load and generation pattern. The rectifier is connected between bus 3 and OR and the inverter is connected between bus 4 and OI. The considerations for this test case are similar to back-to-back VSC-HVDC test case D. C.

C. Point-to-point VSC-HVDC test case:

The test case relates to a simple system where VSC-HVDC link is coordinated with two independent AC source, as shown In Fig.5 Point-to-point VSC-HVDC linking two equivalent AC sub-systems.

The following terms are used:

- (i) Transmission Line 1 and 2: $R_{TL} = 0.05 \text{ p.u.}$, and $X_{TL} = 0.10 \text{ p.u.}$, $B_{TL} = 0.06 \text{ p.u.}$; ;
- (ii) VSC 1 and VSC 2 series resistance and reactance: 0.001 p.u., 0.01 p.u.;
- (iii) For switching loss calculation, VSC 1 and VSC 2 initial shunt conductance $G_{sw} = 0.01 \text{ p.u.}$;
- (iv) LTC 1 and LTC 2 series reactance's: 0.06 p.u.;
- (v) active and reactive power load at bus 2: 1 p.u. and 0.5 p.u.;
- (vi) active and reactive power load at bus 5: 1.5 p.u. and 0.5 p.u.;
- (vii) resistance of DC cable: 0.05 p.u. The considerations for this section are similar to back- to-back case. in 7 iterations ,The solution converges to a tolerance of 10^{-12} . In this voltage at inverter is derived upon convergence of iterative solution. The power flows are shown on Fig.5 where buses 1 and 6 consist of 2.2822 and 0.5434 p.u of active power respectively.

As we know power flows and tap values up to oR are not changed and it is same as back-to-back case. In this active power from slack bus1 gives fewer loads at bus 5 due to power loss which is occurred in resistance. In order to meet demand at bus 5, slack bus at generator 6 consists an additional power. The power loss up to Node OR is same and it changes to the right of bus OR. The power loss occurred in DC cable is 2.5%.In order to supply reactive power load at bus 5, the VSC 2 delivers an 0.6252 p.u.

$$\begin{pmatrix} \bar{I}_{vI} \\ \bar{I}_{oR} \end{pmatrix} \times \begin{pmatrix} \bar{Y}_1(G_{sw} + jm'_{a^2}B_{eq})\bar{Y}_{DC} & -m'_{aI} \angle \phi_I \bar{Y}_1 \bar{Y}_{DC} \\ -m'_{aI} \angle \phi_I \bar{Y}_1 \bar{Y}_{DC} & \bar{Y}_{DC}(m'_{a^2} \bar{Y}_1 + (G_{sw} + jm'_{a^2}B_{eq})) \end{pmatrix} \begin{pmatrix} \bar{V}_{vI} \\ \bar{V}_{oR} \end{pmatrix} \quad (17)$$

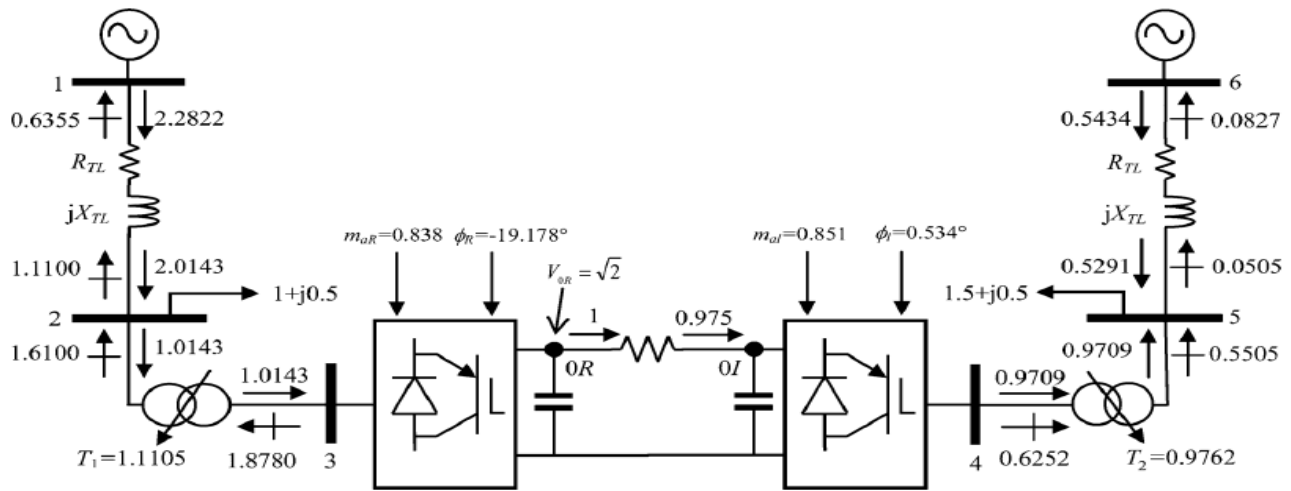


Fig.5 point -to-point VSC-HVDC consists of two equivalent AC sub-systems. The following parameters are used: (i) Transmission Line 1 and 2: $R_{TL}=0.05$ p.u. and $X_{TL}=0.10$ p.u., $B_{TL}= 0.06$ p.u.:(ii) VSC 1 and VSC 2 series resistance and reactance: 0.001 p.u., 0.01 p.u. ; (iii) VSC 1 and VSC 2 initial shunt conductance for switching loss calculation $G_{sw}=0.01$ p.u.; (iv) LTC 1 and LTC 2 series reactance's: 0.06 p.u. ;(v) Active and reactive power load at bus 5: 1.5 p.u. and 0.5 p.u.:(vi) resistance of DC cable: 0.05p.u.

$$G_{eq1} = \frac{1}{\Delta} [(m'_{aI^2}G_1 + G_{sw} + G_{DC})\{G_1(G_{sw} + G_{DC}) - B_1(m'_{a^2}B_{eq} + B_{DC})\} + m'_{aI^2}(B_1 + B_{eq}) + B_{DC}\{B_1(G_{sw} + G_{DC}) + G_1(m'_{aI^2}B_{eq} + B_{DC})\}]$$

$$B_{eq1} = \frac{1}{\Delta} [(m'_{aI^2}G_1 + G_{sw} + G_{DC})\{B_1(G_{sw} + G_{DC}) - G_1(m'_{a^2}B_{eq} + B_{DC})\} + m'_{aI^2}(B_1 + B_{eq}) + B_{DC}\{G_1(G_{sw} + G_{DC}) + B_1(m'_{aI^2}B_{eq} + B_{DC})\}]$$

$$G_{eq1DC} = \frac{1}{\Delta} [(m'_{aI^2}G_1 + G_{sw} + G_{DC})(G_1G_{DC} - B_1B_{DC}) + (m'_{aI^2}(B_1 + B_{eq}) + B_{DC})(B_1G_{DC} + G_1B_{DC})]$$

$$B_{eq1DC} = \frac{1}{\Delta} [(m'_{aI^2}G_1 + G_{sw} + G_{DC})(B_1G_{DC} + G_1B_{DC}) - (m'_{aI^2}(B_1 + B_{eq}) + B_{DC})(G_1G_{DC} - B_1B_{DC})]$$

$$G_{eq0} = \frac{1}{\Delta} [(m'_{aI^2}G_1 + G_{sw} + G_{DC})\{G_{DC}(m_{aI^2}G_1 + G_{sw}) - m_{aI^2}B_{DC}(B_1 + B_{eq}) + (m'_{aI^2}(B_1 + B_{eq}) + B_{DC})\{B_{DC}(m'_{aI^2}G_1 + G_{sw}) + m'_{aI^2}G_{DC}(B_1 + B_{eq})\}]$$

$$B_{eq0} = \frac{1}{\Delta} [(m'_{aI^2}G_1 + G_{sw} + G_{DC})\{B_{DC}(m_{aI^2}G_1 + G_{sw}) + m_{aI^2}G_{DC}(B_1 + B_{eq}) - (m'_{aI^2}(B_1 + B_{eq}) + B_{DC})\{G_{DC}(m'_{aI^2}G_1 + G_{sw}) - m'_{aI^2}B_{DC}(B_1 + B_{eq})\}]$$

$$\Delta = (m'_{af}{}^2 G_1 + G_{sw} + G_{DC})^2 + (m'_{af}{}^2 (B_1 + B_{eq}) + B_{DC})^2$$

Table III Power flow voltage solution

Nodes	1	2	3	OR	OI	4	5	6
V(p.u)	1.02	1.0	1.01	1.4142	1.3788	1.01	1.0	1.02
θ (deg)	0	-14.67	-18.51	-	-	0.03	-3.19	0

Table IV Tap values for the two VSCs and two LTCs

VSC	1	2	LTC	1	2
m_a	0.838 \angle -19.178 ^o	0.831 \angle 0.534 ^o	Tap	1.1105	0.9762

5. Comparison of Back-to-Back and Point-to-Point models. For the sake of completeness the test case is now solved using alternative modeling solution and is contrasted with new model is put forward in this paper. The two methods are compared it against Equivalent voltage source model [7]. The DC voltage, the amplitude modulation ratio and switching power losses are missing in equivalent voltage source model. The equivalent voltage source that represent AC circuit correctly but

where the DC circuit does not exist explicitly. The active and reactive power losses in AC systems 1 and 2 calculated by two models little differ because both models well defined for AC system but difference in power loss since equivalent voltage source model lacks proper DC circuit representation.

The new model yields more realistic not only for switching losses incorporation but it also accurately represents DC voltages than in [6] and with it, more accurate DC current representation.

Table V Power losses incurred by various models

Model	Active power loss(MW)			Reactive power loss(MVAR)		
	Ac1	Ac2	VSC-HVDC	Ac1	Ac2	VSC-HVDC
Back-to-back	26.4	1.49	0.99	73.4	4.45	7.7
Point-to-point	26.5	1.43	2.8	73.4	1.44	23.7

6. Numerical Example of Power Flow Control using One HVDC-VSC

The five-bus system is used to illustrate the power flow control performance of the HVDCVSC

models. This power flow controller may be used to regulate the amount of power flow at their points of connection or even to reverse the direction of power flowing through the controller.

I. HVDC-VSC back-to-back model

The original network is modified to include one back-to-back (BTB) HVDC model to regulate power flow at the points of connection. Take, for instance, the case when the UPFC is installed at the receiving end of line Lake–Main and is set to regulate active and reactive powers flowing from Lake to Main at 40MW and 2MVAR, respectively. The voltage magnitude at bus Lake is controlled at 1 p.u. The back-to-back HVDC model replaces the UPFC used in the test case. As expected, the power flow results for both cases are exactly the same.

II. HVDC-VSC Full model

A different situation arises when the full HVDC-VSC model replaces the combined UPFC–transmission-line model connected between Lake and Main since the DC cable will contain neither the inductance nor the capacitance of the transmission line. In this example, the cable resistance in the DC system is taken to have the same value as the transmission-line resistance in the AC system, which is 1 %. Figure 5.20 shows results for the case when the full HVDC- the AC system, which is 1 %. Figure 5.20 shows results for the case when the full HVDC-VSC is used to control active power flow at Lake at 40MW, and Table 5.9 shows the nodal voltages in the modified network. The data given in function Power Flows Data in Section 4.3.9 is modified to accommodate for the inclusion of the HVDC. For HVDC-BTB the modification is as in Section 5.4.3, and for the HVDC-VSC the transmission line originally connected between Lake and Main is replaced by the HVDC-VSC.

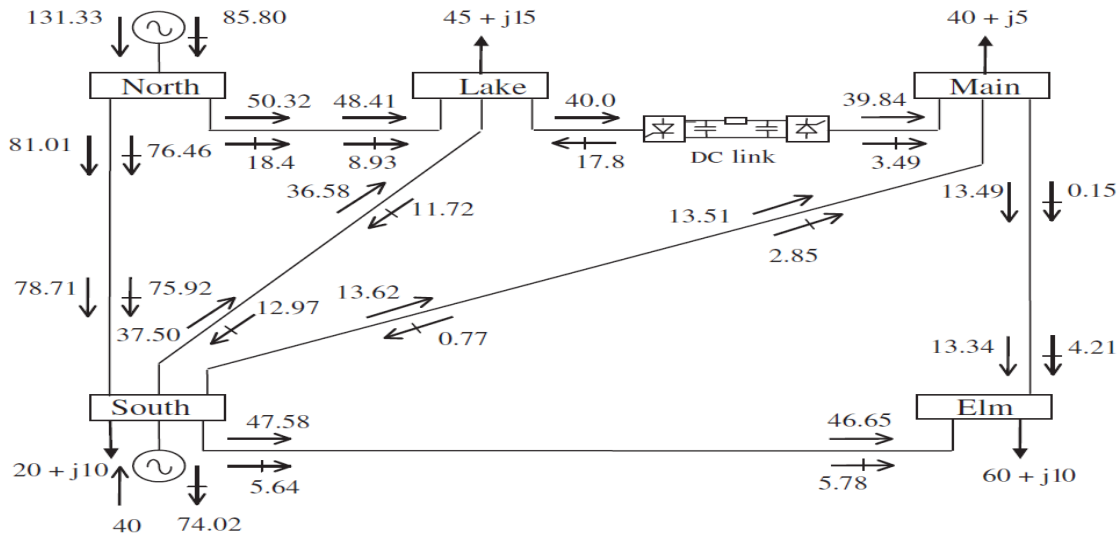


Fig.6 Power flow results in the five-bus network with one full high-voltage direct-current based voltage source converter.

Table VI

Network Bus					
Nodal voltage	North	South	Lake	Main	EIM
Magnitude(p.u.)	1.06	1	1	0.989	0.973
Phase angle(deg)	0	-1.76	-6.01	-3.14	-4.95

Table VII New IEEE 5 Bus system

Model	Active power loss(MW)			Reactive power loss(MVAR)		
	Ac1	Ac2	VSC-HVDC	Ac1	Ac2	VSC-HVDC
Model	7.2	0	0.14	200	5.8	29.9

7. Conclusion:

A new model is suitable for fundamental frequency operation of VSC-HVDC links using Newton-Raphson power flows solutions has been introduced. The back-to-back and the point-to-point configurations have received attention. This model shifts in the way fundamental frequency, Positive sequence modeling. In new model the rectifier and inverter is treated as compound transformer devices In which certain control properties of PWM inverters introduced. Such as DC-to-DC converters linked. The switching and ohmic losses are all represented in the new VSC-HVDC model. Comparisons with available models show that the new model yields similar results to a model of IEEE5 bus system. However, switching power losses do exist in practical VSCs and only the new VSC-HVDC model consists of such losses, hence, the two VSC-HVDC models yield different amount of power loss when realistic conditions are taken into account. Based on reliability towards the convergence, all three VSC-HVDC models converge reliable—they exhibit quadratic convergence

characteristics. This model has been tested in a simple system for ease of reproduction by interested parties. This new model is tested with IEEE5 bus system.

REFERENCES

[1] A New VSC-HVDC Model for Power Flows Using the Newton-Raphson Method Enrique Acha, Senior Member, IEEE, Behzad Kazemtabrizi, Student Member, IEEE, and Luis M. Castro, Student Member, IEEE.

[2] J. Arrillaga, High Voltage Direct Current Transmission, IET, 1998.

[3] G. Asplund, "Application of HVDC light to power system enhancement," in Proc. IEEE PES Winter Meeting, Jan. 2000.

[4] S. Dodds, B. Railing, K. Akman, B. Jacobson, T. Worzyk, and B. Nilsson, "HVDC VSC (HVDC light) transmission—

operating experiences,” in CIGRE 2010, paper B4_203_2010, Paris, France.

[5] C. Angeles-Camacho, O. Tortelli, E. Acha, and C. R. Fuerte-Esquivel, “Inclusion of a high voltage DC-voltage source converter model in a Newton-Raphson power flow algorithm,” *Proc. Inst. Elect. Eng., Gen., Transm., Distrib.*, vol. 150, pp. 691–696, Nov. 2003.

[6] X. P. Zhang, “Multiterminal voltage-sourced converter-based HVDC models for power flow analysis,” *IEEE Trans. Power Syst.*, vol. 19, no. 4, pp. 1877–1884, Nov. 2004.

[7] A. Pizano-Martinez, C. R. Fuerte-Esquivel, H. Ambriz-Perez, and E. Acha, “Modeling of VSC-based HVDC systems for a Newton-Raphson HVDC algorithm,” *IEEE Trans. Power Syst.*, vol. 24, no. 4, pp. 1794–1803, Nov. 2007.

[8] C. A. Cañizares, “Power flow and transient stability models of FACTS controllers for voltage and angle stability studies,” in *Proc. IEEE PES Winter Meeting*, Singapore, Jan. 23–27, 2000, pp. 1447–1454.

[9] J. Beerten, S. Cole, and R. Belmans, “A sequential AC/DC power flow algorithm for networks containing multi-terminal VSC HVDC systems,” in *Proc. IEEE PES General Meeting*, Jul. 2010, pp. 1–7.

[10] J. Beerten, S. Cole, and R. Belmans, “Generalized steady-state VSC MTDC model for sequential AC/DC power flow algorithms,” *IEEE Trans. Power Syst.*, vol. 27, no. 2, pp. 821–829, May 2012.

[11] L. Gengyin, Z. Ming, H. Jie, L. Guaagkai, and L. Haifeng, “Power flow calculation of power systems incorporating VSC-HVDC,” in *Proc. 2004 Int. Conf. Power Syst. Technol.— POWERCON 2004*, Singapore, Nov. 21–24, 2004, pp. 1562–1566.

[12] M. Baradar, M. Ghandhari, and D. V. Hertem, “The modeling of multiterminal VSC-HVDC in power flow calculation using unified methodology,” in *Proc. IEEE PES Int. Conf. Exhib. Innovative Smart Grid Technol. (ISGT Europe)*, Dec. 2011, pp. 1–6.

[13] N. Mohan, T. M. Undeland, and W. P. Robins, *Power Electronics: Converter3, Applications and Design*. New York: Wiley, 2003.